

NATIONAL AERONAUTICS AND SPACE ADMINISTRATION

1005
300 387

TECHNICAL REPORT
R-110

ANALYTICAL METHOD OF APPROXIMATING THE MOTION OF A SPINNING VEHICLE WITH VARIABLE MASS AND INERTIA PROPERTIES ACTED UPON BY SEVERAL DISTURBING PARAMETERS

By JAMES J. BUGLIA, GEORGE R. YOUNG,
JESSE D. TIMMONS, and HELEN S. BRINKWORTH

1961

TECHNICAL REPORT R-110

ANALYTICAL METHOD OF APPROXIMATING THE MOTION OF A SPINNING VEHICLE WITH VARIABLE MASS AND INERTIA PROPERTIES ACTED UPON BY SEVERAL DISTURBING PARAMETERS

**By JAMES J. BUGLIA, GEORGE R. YOUNG,
JESSE D. TIMMONS, and HELEN S. BRINKWORTH**

**Langley Research Center
Langley Air Force Base, Va.**

TECHNICAL REPORT R-110

ANALYTICAL METHOD OF APPROXIMATING THE MOTION OF A SPINNING VEHICLE WITH VARIABLE MASS AND INERTIA PROPERTIES ACTED UPON BY SEVERAL DISTURBING PARAMETERS

By JAMES J. BUGLIA, GEORGE R. YOUNG, JESSE D. TIMMONS, and HELEN S. BRINKWORTH

SUMMARY

An analytical method is presented which approximates the flight-path deviation of a variable-mass, variable-inertia, spin-stabilized vehicle under the influence of (a) initial pitching motions, (b) thrust misalignments, and (c) principal-axis misalignment, or dynamic unbalance. This method includes a first-order analysis of the effect of jet damping on the resulting flight path.

An extensive analysis was carried out on an IBM 704 electronic data processing machine, by integrating numerically the six-degree-of-freedom equations of motion of a thrusting body with variable mass and inertia. This computer analysis was intended to act as a check on the method developed herein, and also to present other investigators with exact numerical answers with which to compare their own results. The results from the analytical solution are compared with the results from the numerical integration, and the results are found to agree well in all cases where no large change in inertia ratio was involved.

The results are presented in terms of the angular deviation in space of the velocity vector from its undisturbed orientation, as a function of spin rate, for each of the disturbing parameters. It is believed that this velocity-vector deviation as a function of spin rate is a much more intuitive indication of the dispersion than the body attitude in space, which is the most frequently used parameter in spin-stabilization discussions.

INTRODUCTION

With the fairly recent advent of very-high-altitude rocket vehicles, the engineer has become faced with the difficult problem of adequately

stabilizing his vehicle in the region where the atmosphere is so thin that conventional aerodynamic controls are rendered useless. One possible means of stabilization is the use of reaction controls in place of the aerodynamic controls. However, in view of the diminutive size of some of the present-day probes and satellite injection stages, a control system of this type would impose a severe weight penalty on this final stage. Hence, some other means of pitch and yaw attitude stabilization must be considered.

Ballisticians have long known that a spinning shell deviates from a predetermined flight path much less than a nonspinning shell. It thus seems natural to attempt to attitude stabilize a rocket vehicle by spinning it and, indeed, this method has been successfully used already in the Vanguard, Explorer, and Pioneer vehicles, and on Scout and other vehicles currently being designed. Spin, however, is not a cure-all: spinning a vehicle gives it a constant attitude in inertial space, but not stability along the constantly changing tangent to the flight path. Hence, **if a large change in flight-path angle is involved**, the method of spin stabilization may not be applicable. Spin stabilization is very effective, however, in the case of a satellite launcher where the last stage, the injection stage, is fired at nearly horizontal flight-path and attitude angles and it is desired to burn out this stage in such a manner that the final velocity vector will be nearly horizontal.

Some investigators in this field (for example, refs. 1 and 2) have chosen as a criterion for spin stabilization the attitude of the body, defined by the two Euler angles in pitch and yaw. It is felt,

however, that a knowledge of the vehicle attitude alone is not the best criterion for determining the effects of various extraneous forces, because the attitude alone does not indicate the final orientation of the velocity vector at stage burnout. This velocity-vector orientation is believed to be a better indication of the dispersion effects sought. Consequently, the data presented herein are given as deviation of the velocity vector from its undisturbed orientation as a function of spin rate for several external disturbing forces.

The two methods in most general use for determining dispersion of a spinning vehicle, with the body attitude as a criterion, are the methods of Nicolaides (ref. 1) and Jarmolow (ref. 2). Nicolaides determines the dispersion in terms of angle of attack α and angle of sideslip β . His parameter is essentially $\sqrt{\alpha^2 + \beta^2}$. He also includes aerodynamic effects, which are neglected here. However, he considers the vehicle mass and moments of inertia, as well as the applied moment and forward velocity, to be constants. His results, therefore, cannot be used to study the dispersion of a spinning rocket during its thrusting phase.

Jarmolow, on the other hand, considers the case of variable mass, moments of inertia, and applied moment; but he discusses only the body attitude. Also, analytical results are given only for the pitch and yaw rates in a body-axis system. Numerical integration must still be used to find the pitch and yaw Euler angles.

The method presented herein utilizes exponential approximations for the variation of the ratio of the applied moment to the pitch moment of inertia, and for the ratio of thrust to linear momentum, which appears as a parameter in the translation equations. These approximations make possible analytical solutions for pitch and yaw Euler angles, and also expressions defining the angular deviations of the velocity vector. These expressions include linear damping in pitch and yaw. The following additional assumptions are made: the ratio of roll inertia to pitch inertia is constant; the vehicle is rigid and has rotational symmetry; there is no roll moment; only small angles are considered; the motion takes place in a vacuum. This study was initiated to determine the effect of various disturbing parameters on the flight path of a solid-propellant rocket motor similar to the final stage of the Scout.

SYMBOLS

A, B, D, E	constants
c'	pitch and yaw damping coefficient, ft-lb-sec
$c = \frac{c'}{I}, 1/\text{sec}$	
$C_1, C_2, \bar{C}_1, \bar{C}_2$	constants
\mathbf{H}_b	angular-momentum vector of vehicle with respect to center of gravity in x_b, y_b, z_b coordinate system, slug-ft ² /sec
\mathbf{H}_c	angular-momentum vector of vehicle with respect to center of gravity in x_c, y_c, z_c coordinate system, slug-ft ² /sec
\mathbf{H}_T	angular-momentum vector of vehicle and jet with respect to center of gravity in x_c, y_c, z_c coordinate system, slug-ft ² /sec
$\mathbf{i}_b, \mathbf{j}_b, \mathbf{k}_b$	unit vectors along the $X_b, Y_b,$ and Z_b -axis, respectively
$\mathbf{i}_c, \mathbf{j}_c, \mathbf{k}_c$	unit vectors along the $X_c, Y_c,$ and Z_c -axis, respectively
I_X, I_Y, I_Z	vehicle moments of inertia about $X_b, Y_b,$ and Z_b -axis, respectively, slug-ft ²
I	I_Y or I_Z (where $I_Y = I_Z$), slug-ft ²
I_{YZ}, I_{XZ}, I_{XY}	vehicle products of inertia about $X_b, Y_b,$ and Z_b -axis, respectively, slug-ft ²
k, k_1, k_2, \bar{k}	constants
l	length from vehicle center of gravity to nozzle exit plane, ft
\mathbf{M}	disturbing-moment vector, $M_X \mathbf{i}_c + M_Y \mathbf{j}_c + M_Z \mathbf{k}_c$, ft-lb
M	magnitude of disturbing moment, ft-lb
m	mass of vehicle, slugs
m_u	element of mass, slugs
$M_u = \frac{M}{I}$ at $t=0, 1/\text{sec}^2$	
$n = \frac{I_X}{I} \omega_0$, radians/sec	
p, q, r	angular-velocity components of vehicle about $X_b, Y_b,$ and Z_b -axis, respectively, radians/sec unless otherwise indicated
\mathbf{r}_e	distance from center of gravity to jet exit, $r_{e,x} \mathbf{i}_c + r_{e,y} \mathbf{j}_c + r_{e,z} \mathbf{k}_c$, ft
r_e	magnitude of \mathbf{r}_e , ft

t	time, sec
T	thrust, lb
\mathbf{V}	vehicle velocity vector, ft/sec
V	magnitude of \mathbf{V} , ft/sec
\mathbf{V}_e	jet exhaust velocity, $V_{e,x}\mathbf{i}_c + V_{e,y}\mathbf{j}_c + V_{e,z}\mathbf{k}_c$, ft/sec
V_e	magnitude of \mathbf{V}_e , ft/sec
x_b, y_b, z_b	coordinates measured along body X_b , Y_b , and Z_b -axis, respectively
X_b, Y_b, Z_b	body-fixed system of orthogonal axes, origin at body center of gravity
x_c, y_c, z_c	coordinates measured along X_c , Y_c , and Z_c -axis, respectively
X_c, Y_c, Z_c	system of orthogonal axes which pitches and yaws with vehicle but does not roll, origin at body center of gravity
x_u, y_u	coordinates of element of mass causing dynamic unbalance
α	angle of attack, radians
β	angle of sideslip, radians
γ	orientation of velocity vector in vertical plane, radians
δ	thrust misalignment angle, radians (except as noted)
ϵ	principal-axis misalignment angle, radians (except as noted)
λ	orientation of velocity vector in horizontal plane, radians
σ	total orientation of velocity vector, radians (except as noted)
θ	pitch Euler angle, radians (except as noted)
ψ	yaw Euler angle, radians (except as noted)
ω_c	angular velocity of nonrolling system in inertial space, $\omega_{Yc}\mathbf{j}_c + \omega_{Zc}\mathbf{k}_c$, radians/sec
ω_{Yc}, ω_{Zc}	components of ω_c along Y_c - and Z_c -axis, respectively, radians/sec
Subscripts:	
o	denotes quantity at zero time
X, Y, Z	components parallel to X_b , Y_b , and Z_b -axis, respectively
X_c, Y_c, Z_c	components parallel to X_c , Y_c , and Z_c -axis, respectively

A dot over a quantity denotes differentiation with respect to time.

ANALYSIS

The mathematical analysis of a spinning rocket differs in several respects from that of a spinning projectile. In the first place, the rocket has mass and inertia properties which vary with time, whereas those of a spinning projectile are constant. Secondly, the rocket can have a moment due to a thrust misalignment. This moment, which is fixed to the spinning vehicle, gives rise to motions not found in the analysis of projectile motion. The motions due to an initial pitch or yaw rate and a dynamic unbalance are common to both types of bodies, but the analysis becomes more involved when a variable-property vehicle is dealt with.

The equations of motion programed on the IBM 704 electronic data processing machine for comparison purposes in this study are the standard six-degree-of-freedom equations found in most aeronautical textbooks (for example, ref. 3). The equations programed, along with the various transformations that were used, are presented for reference in the appendix.

An approximate analytical method of predicting the deviation of the velocity vector due to the effects of thrust misalignment, initial pitch rate, and principal-axis misalignment will be developed in this section. Two coordinate systems will be used in this analysis. The first (x_b, y_b, z_b) is a body-fixed coordinate system with axes fixed at the center of gravity of the vehicle and the coordinate x_b extending along the body longitudinal axis. The second coordinate system (x_c, y_c, z_c) , in which the equations of motion will be derived, is referred to a body-fixed system of axes which can pitch and yaw with the vehicle but does not roll with it. The two sets of coordinate axes are aligned at $t=0$. (See fig. 1.) The pitch Euler angle θ and the yaw Euler angle ψ are assumed to be small so that the order of the Euler rotation is immaterial. This assumption of small angles simplifies the integration for γ and λ , the flight-path angles in the vertical and horizontal planes, respectively, and also permits these flight-path angles to combine vectorially to give σ , the angle between the velocity vector and some fixed reference line, taken here as the longitudinal axis of the vehicle at zero time.

The angular-momentum vector of the vehicle in the x_b, y_b, z_b system instantaneously fixed in

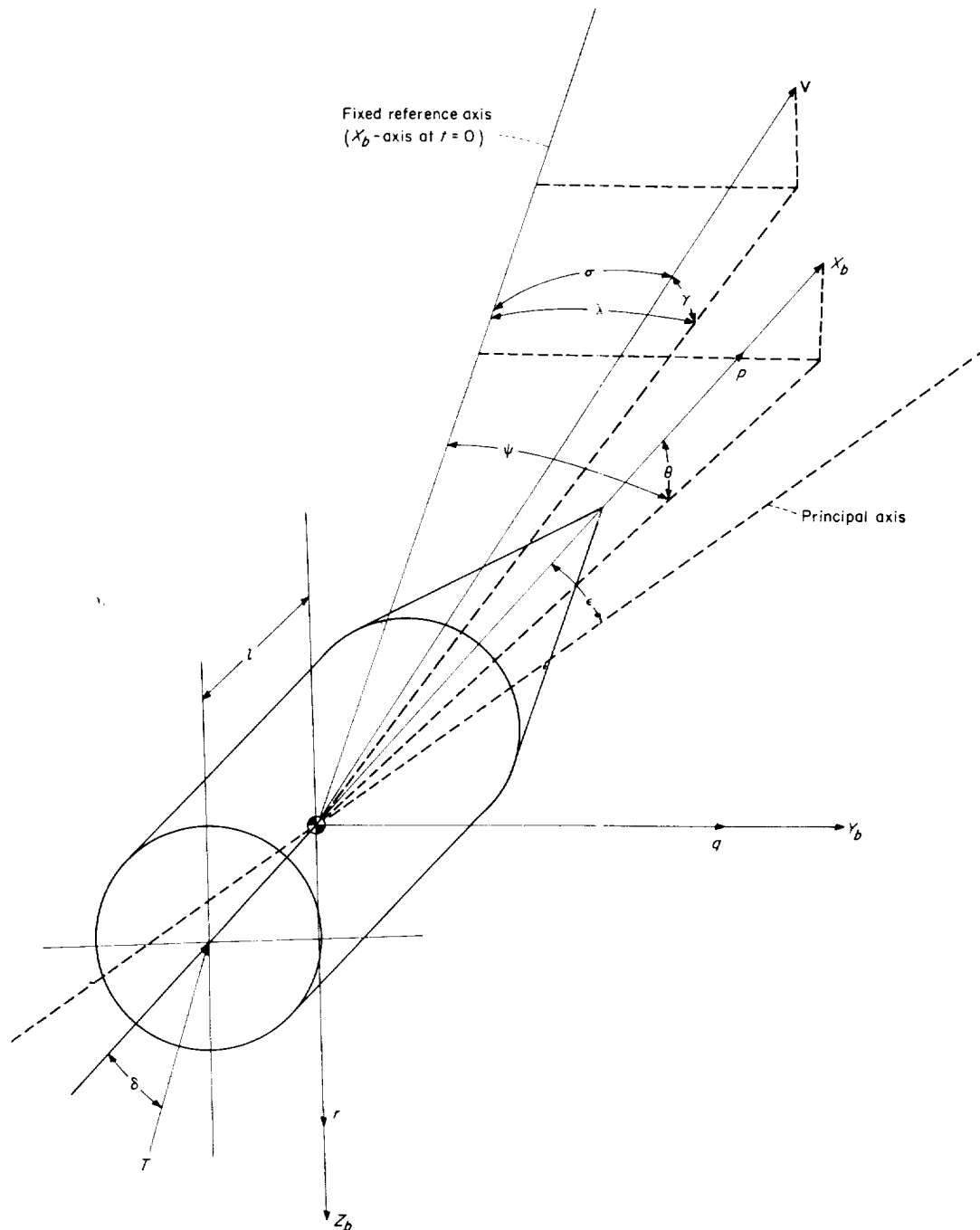


FIGURE 1.—Coordinate system and definition of symbols used in analytical development.

inertial space can be written

$$\mathbf{H}_b = (I_X p - I_{XY} q - I_{XZ} r) \mathbf{i}_b + (I_Y q - I_{YZ} r - I_{XY} p) \mathbf{j}_b \\ + (I_Z r - I_{XZ} p - I_{YZ} q) \mathbf{k}_b \quad (1)$$

Now, in the nonrolling system (x_c, y_c, z_c) , which has angular velocity in inertial space,

$$\boldsymbol{\omega}_c = (0, \omega_{Yc}, \omega_{Zc}) = \omega_{Yc} \mathbf{j}_c + \omega_{Zc} \mathbf{k}_c \quad (2)$$

The equation of motion about the vehicle center

of gravity is

$$\frac{d\mathbf{H}_T}{dt} = \mathbf{M} \quad (3)$$

The rate of change of angular momentum with respect to the vehicle center of gravity including jet effect is

$$\frac{d\mathbf{H}_T}{dt} = \frac{d\mathbf{H}_c}{dt} + \boldsymbol{\omega}_c \times \mathbf{H}_c + \dot{m} \mathbf{r}_c \times (\boldsymbol{\omega}_c \times \mathbf{r}_c - \mathbf{V}_c) \quad (4)$$

where $\boldsymbol{\omega}_c \times \mathbf{H}_c$ takes into account the rotation of the coordinate system.

It is usually conventional in missile work to choose the body axes as principal axes and to assume a symmetrical vehicle, so that

$$\left. \begin{aligned} I_Y = I_Z = I \\ I_{XY} = I_{YZ} = I_{XZ} = 0 \end{aligned} \right\} \quad (5)$$

With these assumptions, equation (1) may be written in the nonrolling system as

$$\mathbf{H}_c = I_X p \mathbf{i}_c + I_Y r \mathbf{j}_c + I_Z \dot{r} \mathbf{k}_c \quad (6)$$

If the further assumptions are made that the jet is located on the X_c -axis and the jet exit velocity relative to the nozzle exit is directed along the negative X_c -axis, then

$$\left. \begin{aligned} V_{e,Xc} = V_e \\ V_{e,Yc} = V_{e,Zc} = 0 \end{aligned} \right\} \quad (7)$$

and

$$\left. \begin{aligned} r_{e,Xc} = r_e \\ r_{e,Yc} = r_{e,Zc} = 0 \end{aligned} \right\} \quad (8)$$

Expansion of equation (3), with the aid of substitutions from equations (2), (4), and (6), yields

$$\begin{aligned} (I_X \dot{p} + \dot{I}_X p) \mathbf{i}_c + (I_Y \dot{r} + \dot{I}_Y r + I_X p \omega_{Zc} + \dot{m} r_e^2 \omega_{Yc}) \mathbf{j}_c \\ + (I_Z \dot{r} + \dot{I}_Z r - I_X p \omega_{Yc} + \dot{m} r_e^2 \omega_{Zc}) \mathbf{k}_c = \mathbf{M} \end{aligned} \quad (9)$$

If damping in roll is neglected (that is, if $\dot{I}_X = 0$), equation (9) becomes, in component form,

$$I_X \dot{p} = M_X \quad (10a)$$

$$I_Y \dot{r} + I_X p \omega_{Zc} + c' \omega_{Yc} = M_Y \quad (10b)$$

$$I_Z \dot{r} - I_X p \omega_{Yc} + c' \omega_{Zc} = M_Z \quad (10c)$$

where

$$c' = \dot{m} r_e^2 + \dot{I}$$

The quantity $c'/I (= c)$ will be considered constant for this analysis.

If the assumptions are made that the disturbing moment lies in the vertical plane at zero time and that there is no moment about the roll axis, then

$$\left. \begin{aligned} M_X &= 0 \\ M_Y &= M \cos pt \\ M_Z &= M \sin pt \end{aligned} \right\} \quad (11)$$

and equations (10) become

$$I_X \dot{p} = 0 \quad (12a)$$

$$I_Y \dot{r} + I_X p \omega_{Zc} + c' \omega_{Yc} = M \cos pt \quad (12b)$$

$$I_Z \dot{r} - I_X p \omega_{Yc} + c' \omega_{Zc} = M \sin pt \quad (12c)$$

Equation (12a) immediately shows that

$$p = \text{Constant} = p_o$$

Let

$$\frac{I_X}{I} p_o = n \quad (13)$$

and

$$\frac{M}{I} = M_o e^{kt} \quad (14)$$

It is assumed that the ratio I_X/I is constant; M_o and k are also constants, found by fitting an exponential to the function M/I as shown in equation (14). Then equations (12b) and (12c) become

$$\dot{\omega}_{Yc} + n \omega_{Zc} + c \omega_{Yc} = M_o e^{kt} \cos p_o t \quad (15a)$$

$$\dot{\omega}_{Zc} - n \omega_{Yc} + c \omega_{Zc} = M_o e^{kt} \sin p_o t \quad (15b)$$

These equations can be integrated simply, and with the initial conditions $\omega_{Yc}(0) = \omega_{Yc,o}$, $\omega_{Zc}(0) = 0$ give

$$\begin{aligned} \omega_{Yc} = (\omega_{Yc,o} - C_2) e^{-ct} \cos nt - C_1 e^{-ct} \sin nt \\ + C_2 e^{kt} \cos p_o t + C_1 e^{kt} \sin p_o t \end{aligned} \quad (16a)$$

$$\begin{aligned} \omega_{Zc} = (\omega_{Yc,o} - C_2) e^{-ct} \sin nt + C_1 e^{-ct} \cos nt \\ + C_2 e^{kt} \sin p_o t - C_1 e^{kt} \cos p_o t \end{aligned} \quad (16b)$$

where

$$C_1 = \frac{M_o(p_o - n)}{(c + k)^2 + (p_o - n)^2} \quad (17a)$$

$$C_2 = \frac{M_0(c+k)}{(c+k)^2 + (p_0-n)^2} \quad (17b)$$

Now, by virtue of the original assumption that the pitch and yaw motions are small, and as a consequence of the coordinate system used, the following expressions can be written:

$$\theta = \int \omega_Y dt \quad (18a)$$

$$\psi = \int \omega_Z dt \quad (18b)$$

Substitution of equations (16a) and (16b) into these integrals with the initial conditions $\theta(0) = \psi(0) = 0$ gives

$$\theta = A(e^{kt} \cos p_0 t - 1) + B e^{kt} \sin p_0 t - D(e^{-ct} \cos nt - 1) + E e^{-ct} \sin nt \quad (19a)$$

$$\psi = A e^{kt} \sin p_0 t - B(e^{kt} \cos p_0 t - 1) - D e^{-ct} \sin nt + E(e^{-ct} \cos nt - 1) \quad (19b)$$

where

$$A = \frac{C_2 k - C_1 p_0}{k^2 + p_0^2} \quad (20a)$$

$$B = \frac{C_2 p_0 + C_1 k}{k^2 + p_0^2} \quad (20b)$$

$$D = \frac{c(\omega_{Yc,0} - C_2) - n C_1}{c^2 + n^2} \quad (20c)$$

$$E = \frac{n(\omega_{Yc,0} - C_2) + c C_1}{c^2 + n^2} \quad (20d)$$

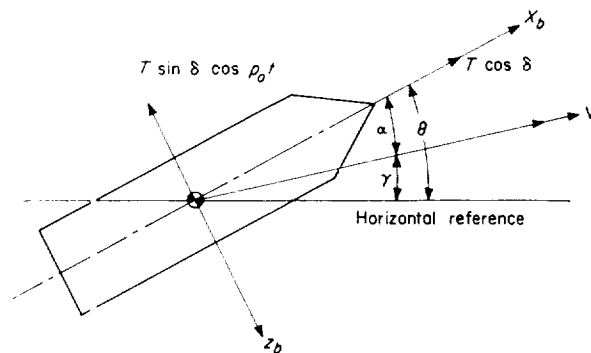
These equations give time histories of the body attitude angles in an inertial coordinate system taken to be coincident with the body coordinate system at zero time. These angles θ and ψ are the angles commonly used to discuss the effects of spin on the stability or dispersion of a vehicle. However, body attitude alone does not adequately describe the complete motion in space. The actual dispersion of the vehicle, defined herein as the angle between the velocity vector at zero time and the velocity vector at burnout, is a much more meaningful parameter because it depends on the translation of the vehicle, and hence on the quantities which define its translation history, as well as on the rotational parameters. The preceding argument can be substantiated from physical

considerations. The equations defining the rotational motion of the vehicle are completely independent of the translational motion. (See, for example, eqs. (A1) to (A6).) Hence, for given inertia characteristics, spin rate, and disturbance, the rotational motion of the vehicle is completely defined. Now, in order to get the actual translation in space, the body attitude parameters must be combined with the translation parameters; for example, equations relating quantities such as thrust and mass ratio are integrated to give the translational motion. As an illustration, it is certainly possible to have a spinning vehicle pointing vertically upward and moving horizontally at ignition. Then as the motor fires the velocity vector climbs above the horizontal. Thus, the final direction of the velocity vector has changed—the dispersion as defined here is reduced—but the body attitude has remained constant. An effect such as this one is not evident when only the rotational motion is defined.

In order to determine γ , the orientation of the velocity vector in the vertical plane, reference is made to the normal equation of motion of figure 2(a). Since $\alpha = \theta - \gamma$, if only small angles are taken it to account this equation becomes

$$\frac{d\gamma}{dt} + \frac{T}{mV} \gamma = \frac{T}{mV} \theta + \frac{T}{mV} \delta \cos p_0 t \quad (21)$$

In a similar manner a differential equation for λ ,



(a)

$$mV\dot{\gamma} = T \sin \delta \cos p_0 t \cos \alpha + T \cos \delta \sin \alpha$$

$$mV\dot{\gamma} = T \delta \cos p_0 t + T(\theta - \gamma)$$

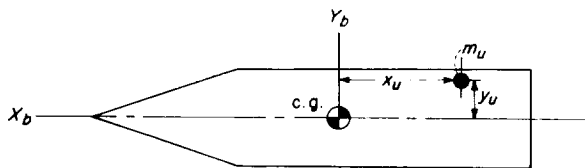
(a) Vertical plane.

FIGURE 2.—Equations of motion.

Then, because of the assumption of small angles, γ and λ can be combined vectorially to give σ , the angle between the fixed reference line and the velocity vector:

$$\sigma = \sqrt{\gamma^2 + \lambda^2} \quad (27)$$

A disturbing parameter consisting of a principal-axis misalignment can be handled in the following manner. Assume that the mass element causing the dynamic unbalance can be placed off the center line of the vehicle a distance y_u from the center of rotation, and that it has a mass m_u , as in sketch 1. The moment about the center



Sketch 1.

of gravity due to this mass element is

$$M = p_o^2 x_u y_u m_u \quad (28)$$

Now, the product of inertia due to this mass is

$$I_{XY} = x_u y_u m_u \quad (29)$$

Hence, the moment can be written in terms of the product of inertia:

$$M = p_o^2 I_{XY} \quad (30)$$

It may be desirable to express the product of inertia in terms of the principal-axis misalignment angle ϵ . From the properties of moments of inertia it is known that the angle ϵ between the principal axis and the axis about which the moments and products of inertia are computed is given by

$$\tan 2\epsilon = \frac{2I_{XY}}{I_X - I_Y} \quad (31)$$

If, as will be the usual case, the product-of-inertia term is due to construction technique or placing of instrumentation, the product of inertia will be constant, the small change due to the center-of-gravity shift during burning being neglected. In this case, ϵ will be a function of time. The time history of ϵ can be computed from equation (31) since I_X and I_Y are known at any time. Then

with the assumption $\epsilon \ll 1$, substitution of equation (31) into equation (30) gives

$$\frac{M}{I} = -p_o^2 \epsilon(t) \left(1 - \frac{I_X}{I_Y}\right) \quad (32)$$

If this expression is used in equation (14), and M_u and k are found by a curve fit, solution of equations (25) and (26) will yield histories of γ and λ due to a principal-axis misalignment ϵ .

It should be noted that, to the degree of approximation used herein, the effects of the various disturbing parameters can be combined linearly to yield the total dispersion. For example, equations (25) and (26) may be written as a linear combination of terms each of which is a function of $\omega_{rc,0}$, M_u , or δ but not of any two of the variables.

It should be further noted that, again to the degree of approximation assumed here, the angles γ and λ , and consequently the total dispersion σ , vary linearly with $\omega_{rc,0}$ and M_u , if taken separately, so that it is not necessary to make a separate calculation for each value of moment or pitch rate desired. This linearity is supported by the calculations performed on the IBM 704 computer, as illustrated in several of the figures.

RESULTS AND DISCUSSION

A comparison of the results of the numerical integration (on the IBM 704 computer) of the exact equations of motion given in the appendix with the results of the analytical solutions developed herein is made in figures 3 to 16. The quantities θ , ψ , γ , λ , and σ were calculated from equations (19a), (19b), (25), (26), and (27), respectively. The constants used are given in tables I and II. Figures 7 to 16 are plotted for $t=30$ seconds (burnout). These figures serve a double purpose. Since not everyone has access to an IBM 704 or to a computer of sufficient capability and storage capacity to permit the programming of a problem as complex as a six-degree-of-freedom rigid-body analysis, many investigators have probably developed analytical results without being able to check the accuracy of their methods. Thus, the figures presented can serve to check these methods and indicate regions of validity and applicability. At the same time, the figures serve to illustrate the accuracy of the analytical method developed herein. As can be

TABLE I. PHYSICAL AND PERFORMANCE CHARACTERISTICS OF ROCKET MOTOR USED IN CALCULATIONS

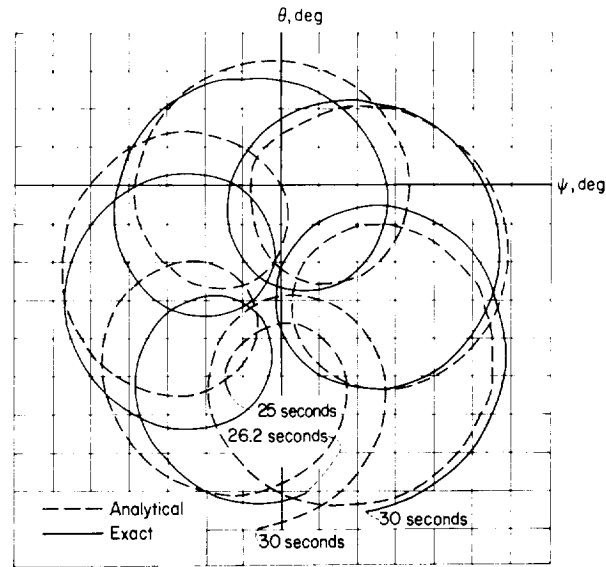
Roll moment of inertia, slug-ft ²	5.25	0.13%
Pitch (yaw) moment of inertia, slug-ft ²	34.15	0.88%
Mass, slugs	18.95	0.48%
Applied moment, ft-lb (δ in radians)	10,710 δ	1500%
Thrust, lb	3,000	
Burning time, sec	30	
Initial velocity, ft/sec	10,000	
Final velocity, ft/sec	19,816	
Computed constants (for 0.10° thrust misalignment):		
k_1	0.01583	
k_2	0.0260	
k_3	0.608	
C_1	1.839	
C_2	0.050	
δ , radians	0.001745	
$\omega_{yc,0}$, radians/sec	0	
I_X/I_Z	0.164	
M_a , 1/sec ²	0.5470	
k	0.0592	

TABLE II. PHYSICAL AND PERFORMANCE CHARACTERISTICS OF SPHERICAL ROCKET MOTOR

Roll moment of inertia, slug-ft ²	333.6	10.0%
Pitch (yaw) moment of inertia, slug-ft ²	403.6	10.0%
Mass, slugs	16.33	0.51%
Thrust, lb	3,466	
Burning time, sec	30	
Moment, ft-lb	54	0.01%
Initial velocity, ft/sec	10,000	
Final velocity, ft/sec	29,950	
Computed constants:		
k_1	0.02125	
k_2	0.0790	
k_3	0.269	
C_1	1.236	
C_2	0.167	
δ , radians	0	
$\omega_{yc,0}$, radians/sec	0	
I_X/I_Z	0.68	
M_a , 1/sec ²	0.0124	
k	0.042	

seen from a general perusal of figures 3 to 15, the accuracy obtained is quite good in the range investigated.

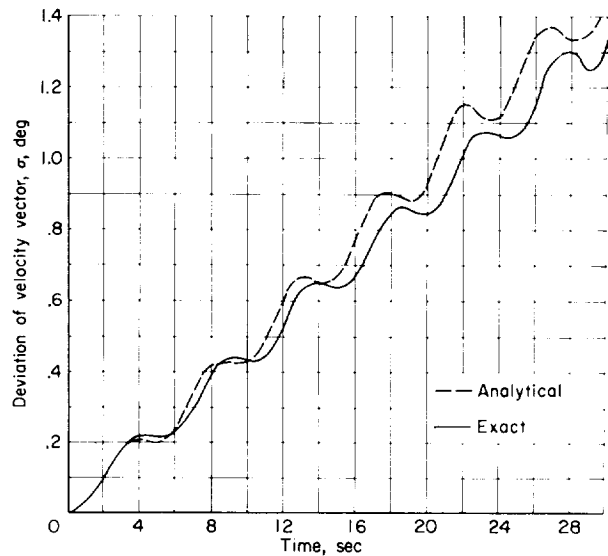
Figure 3 shows the pitch Euler angle θ plotted against the yaw Euler angle ψ , for the last few seconds of burning of the rocket motor, under the action of a moment produced by a thrust misalignment δ of 0.10°. This figure shows, essentially, the attitude of the body in space during this time. It can be seen that, although the analytical method predicts frequencies of nutation and precession which are slightly high, the amplitudes of both

FIGURE 3. Undamped body attitude. $p_a = 80$ rpm; $\delta = 0.10^\circ$.

motions, which are the parameters of primary interest, are predicted rather well. This curve does not include the effect of jet damping.

Figure 4 shows time histories of the deviation of the velocity vector σ . The analytical method predicts results which are slightly conservative.

In figures 5 and 6 are plotted time histories of the pitch Euler angle θ and the yaw Euler angle ψ , respectively. Here it will be noted that, while

FIGURE 4. Deviation of velocity vector as a function of time, for a thrust misalignment angle δ of 0.10°. Undamped body; $p_a = 80$ rpm.

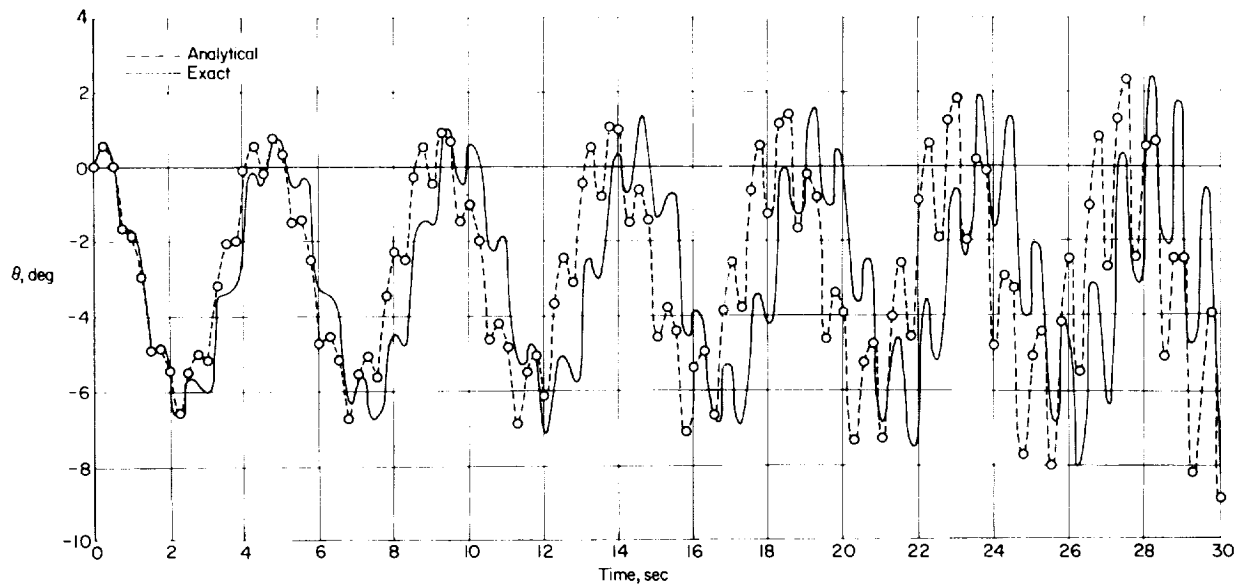


FIGURE 5.—Pitch Euler angle as a function of time. Undamped body; $p_o=80$ rpm; $\delta=0.10^\circ$.

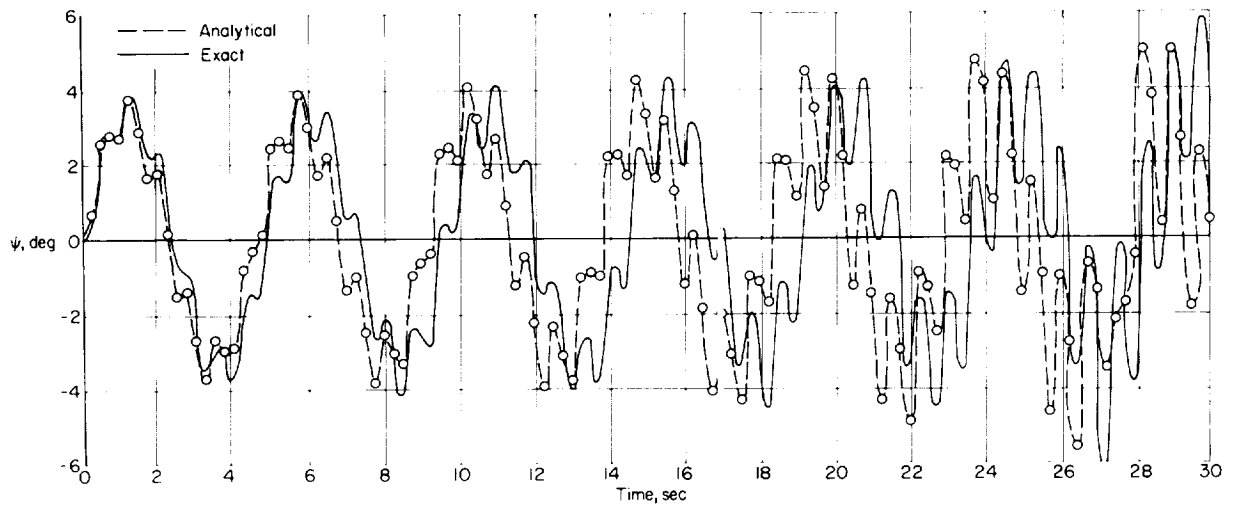


FIGURE 6.—Yaw Euler angle as a function of time. Undamped body; $p_o=80$ rpm; $\delta=0.10^\circ$.

the agreement is only fair (again the frequency is in error), the amplitude of $\sqrt{\theta^2 + \psi^2}$ is in good agreement as seen from figure 3.

Figures 7 to 15 show the effect of spin rate on the deviation of the velocity vector σ for several values of thrust misalignment, principal-axis misalignment, and initial pitch rate. These figures are all plotted for $t = 30$ seconds (burnout), and figures 8, 11, and 14 include the effect of damping in pitch and yaw. Again the analytical results are compared with the machine-integrated results and the agreement is seen to be good in all cases.

The linearity of σ with the magnitude of the disturbing parameters, as predicted by the analytical results, is shown in figures 9, 12, and 15. For the range of the disturbing parameters chosen, this linearity is substantiated by the machine-integrated results. Figures 7 to 15 show that spin is very effective in reducing the effects of thrust misalignment or initial pitch rate, but is completely ineffective in reducing the effects of principal-axis misalignment. The reason for this ineffectiveness is that the higher the spin rate, the greater the disturbing moment due to the dynamic

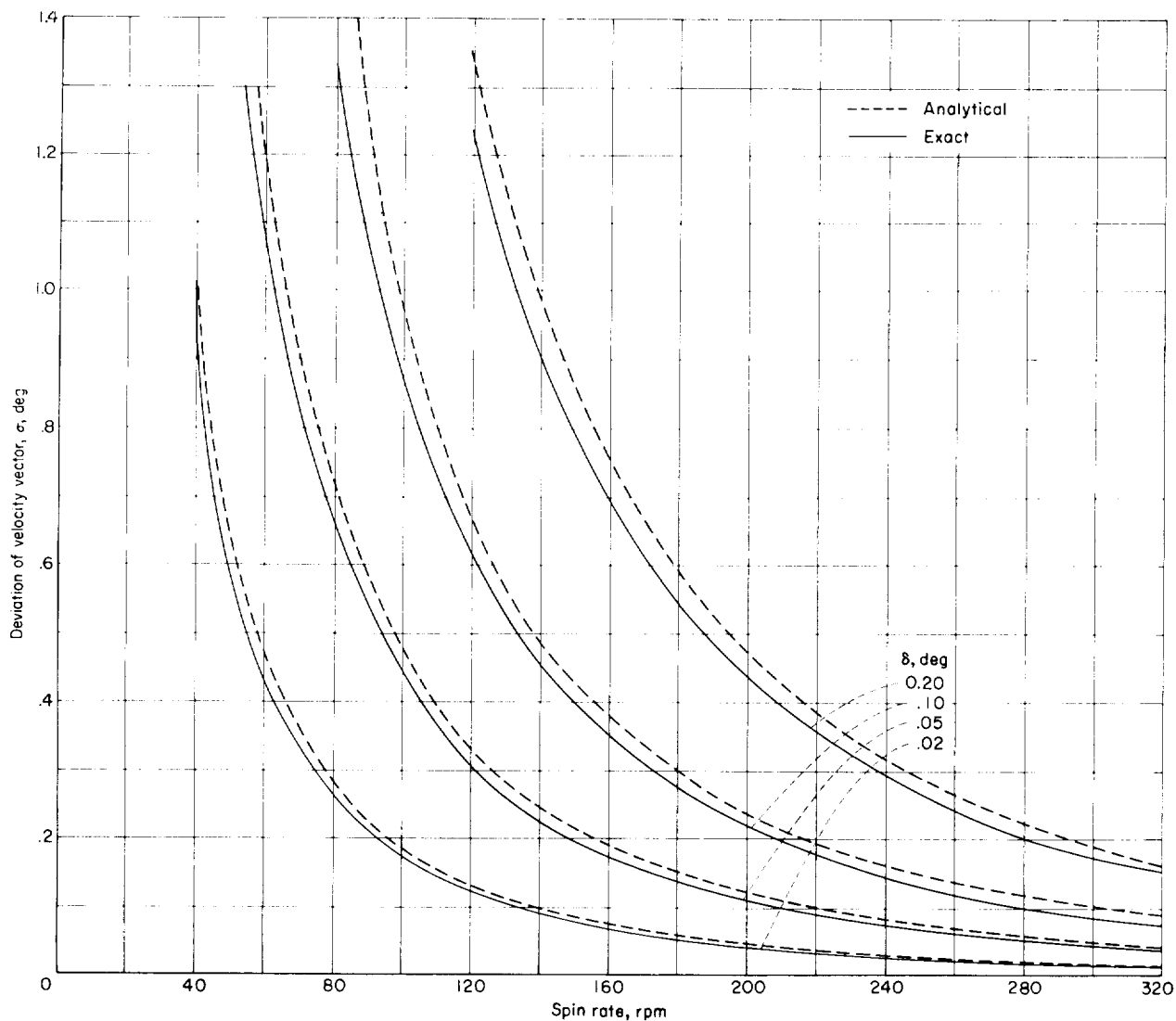


FIGURE 7. Effect of spin rate on the deviation of the velocity vector due to a thrust misalignment angle δ . Undamped body; $t = 30$ seconds (burnout).

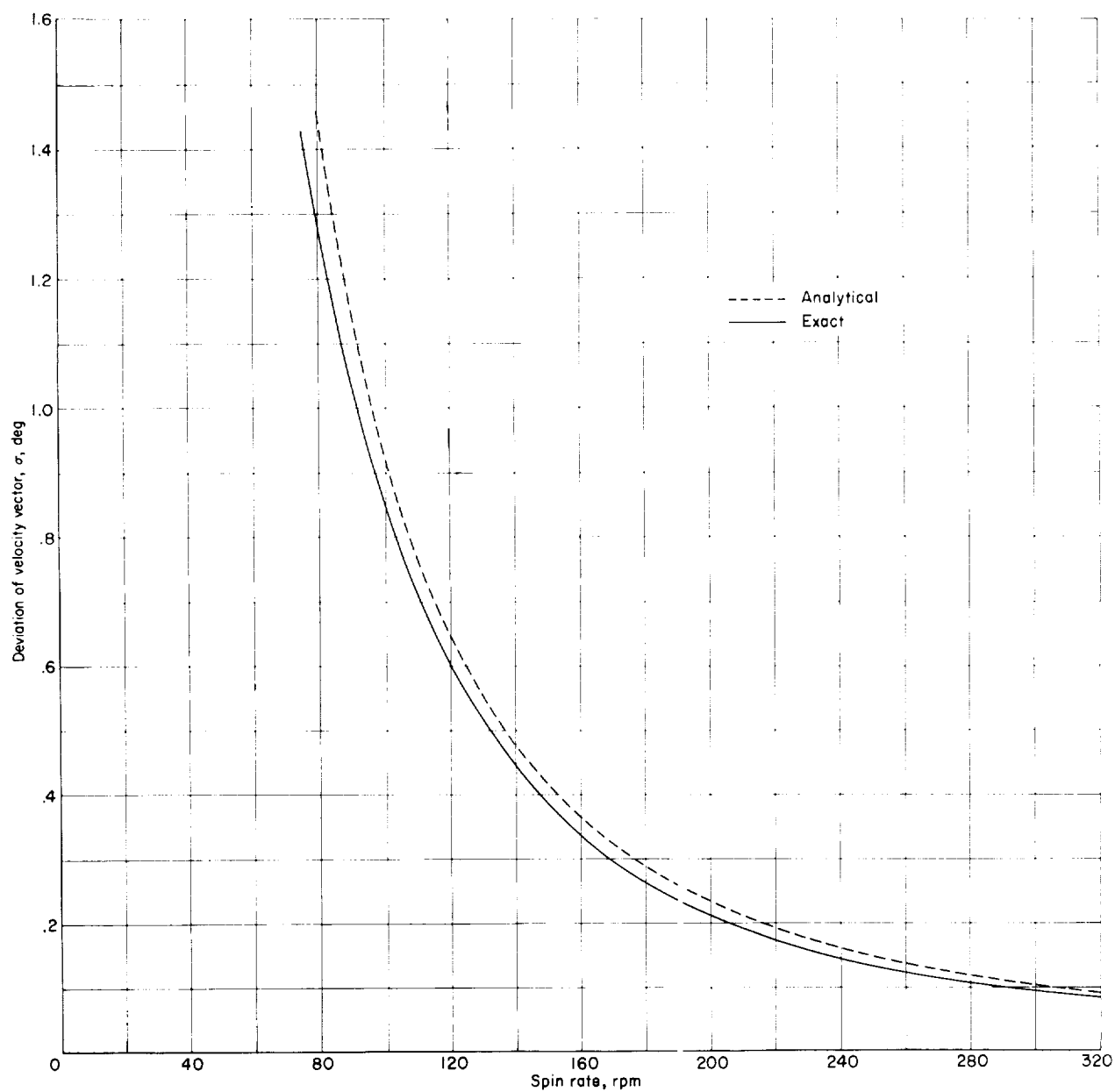


FIGURE 8.—Effect of spin rate on the deviation of the velocity vector due to a thrust misalignment angle δ of 0.10° . Damped body; $t=30$ seconds (burnout).

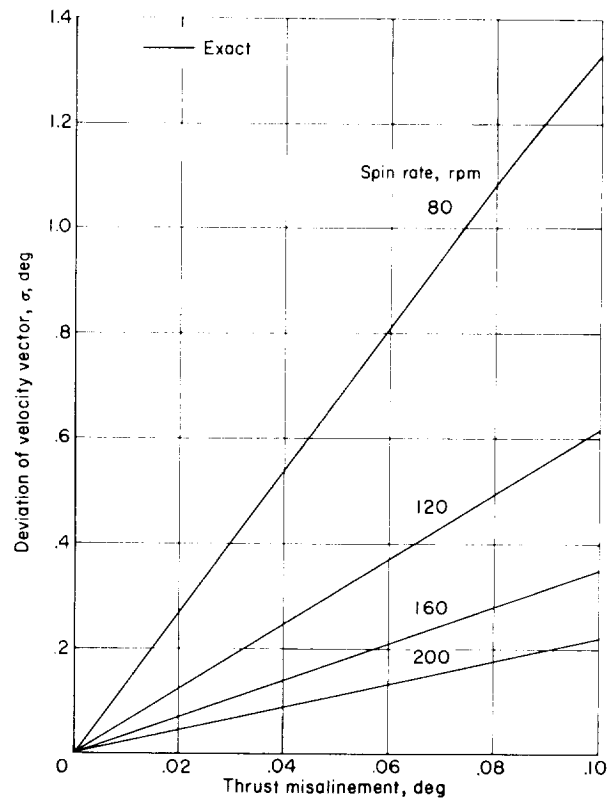


FIGURE 9. Linear effect of thrust misalignment on the deviation of the velocity vector for several spin rates. Undamped body; $t = 30$ seconds (burnout).

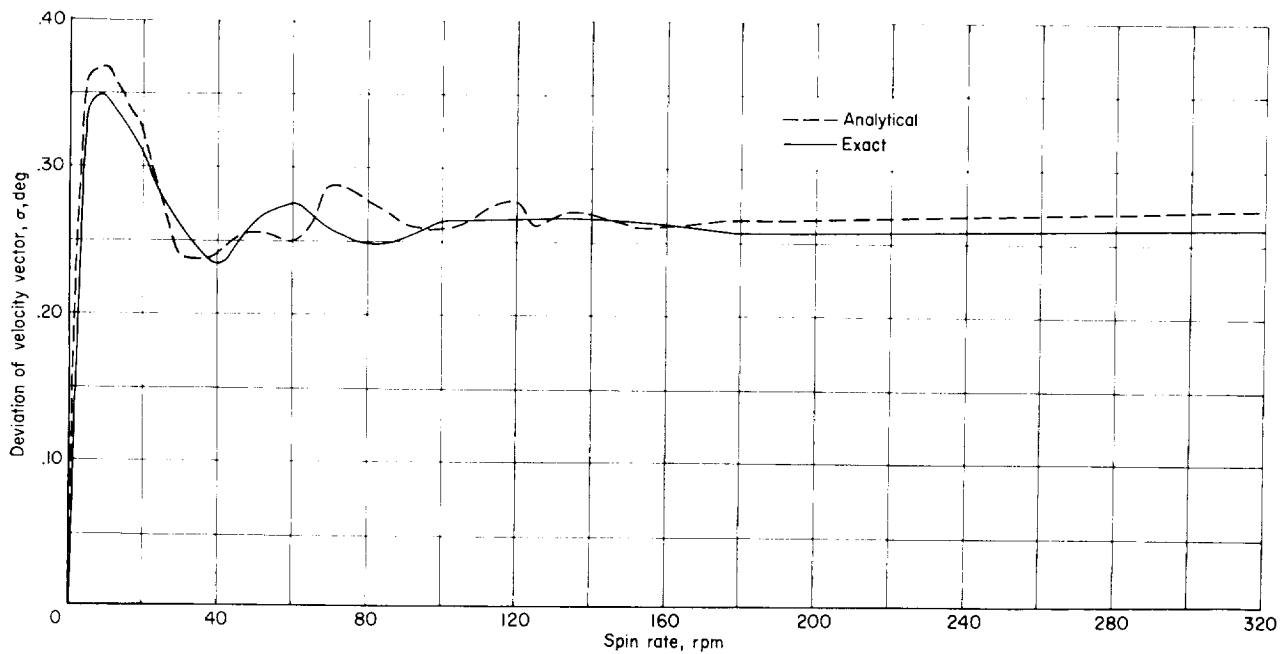


FIGURE 10. Effect of spin rate on the deviation of the velocity vector due to a principal-axis misalignment angle ϵ of 0.10° . Undamped body; $t = 30$ seconds (burnout).

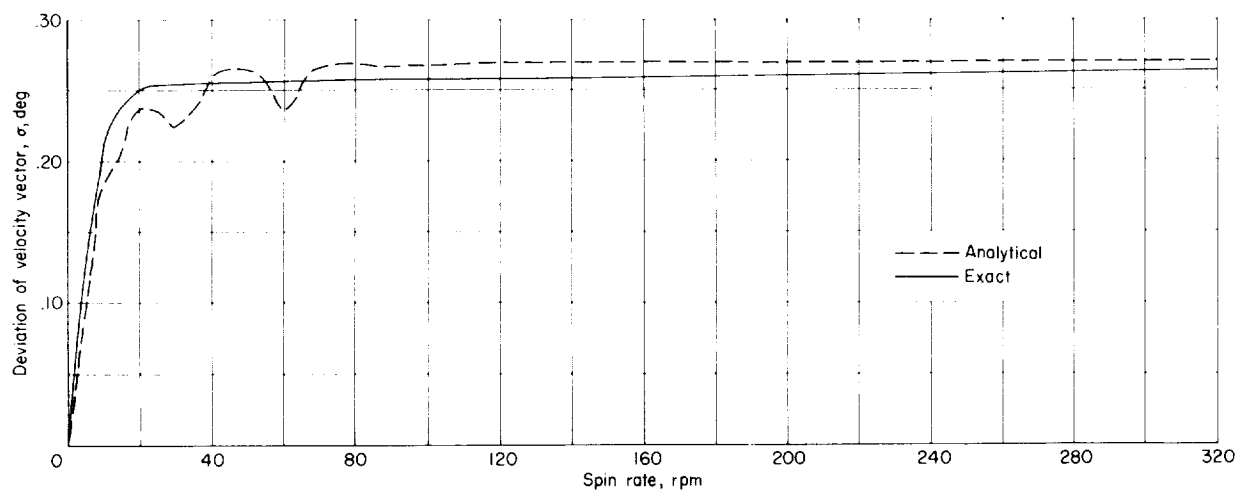


FIGURE 11.— Effect of spin rate on the deviation of the velocity vector due to a principal-axis misalignment angle ϵ of 0.10° . Damped body; $t = 30$ seconds (burnout).

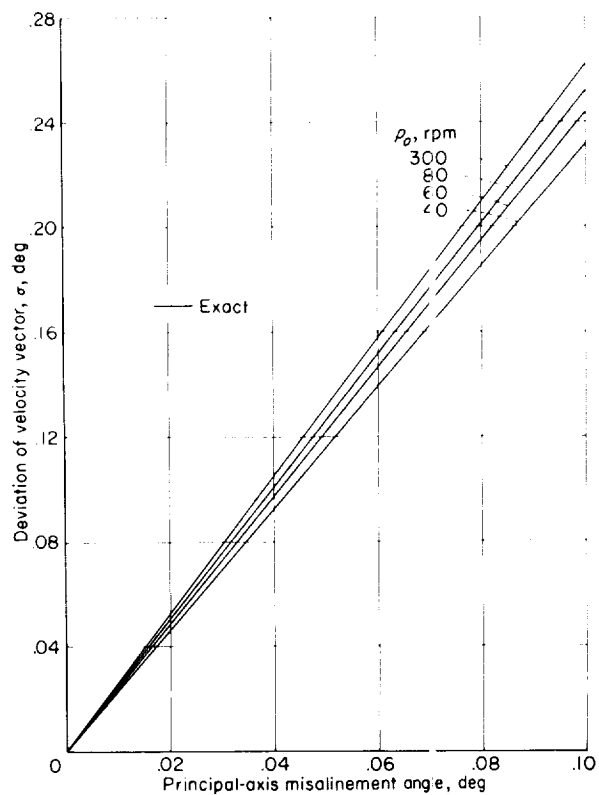


FIGURE 12. Linear effect of principal-axis misalignment on the deviation of the velocity vector for several spin rates. Undamped body; $t = 30$ seconds (burnout).

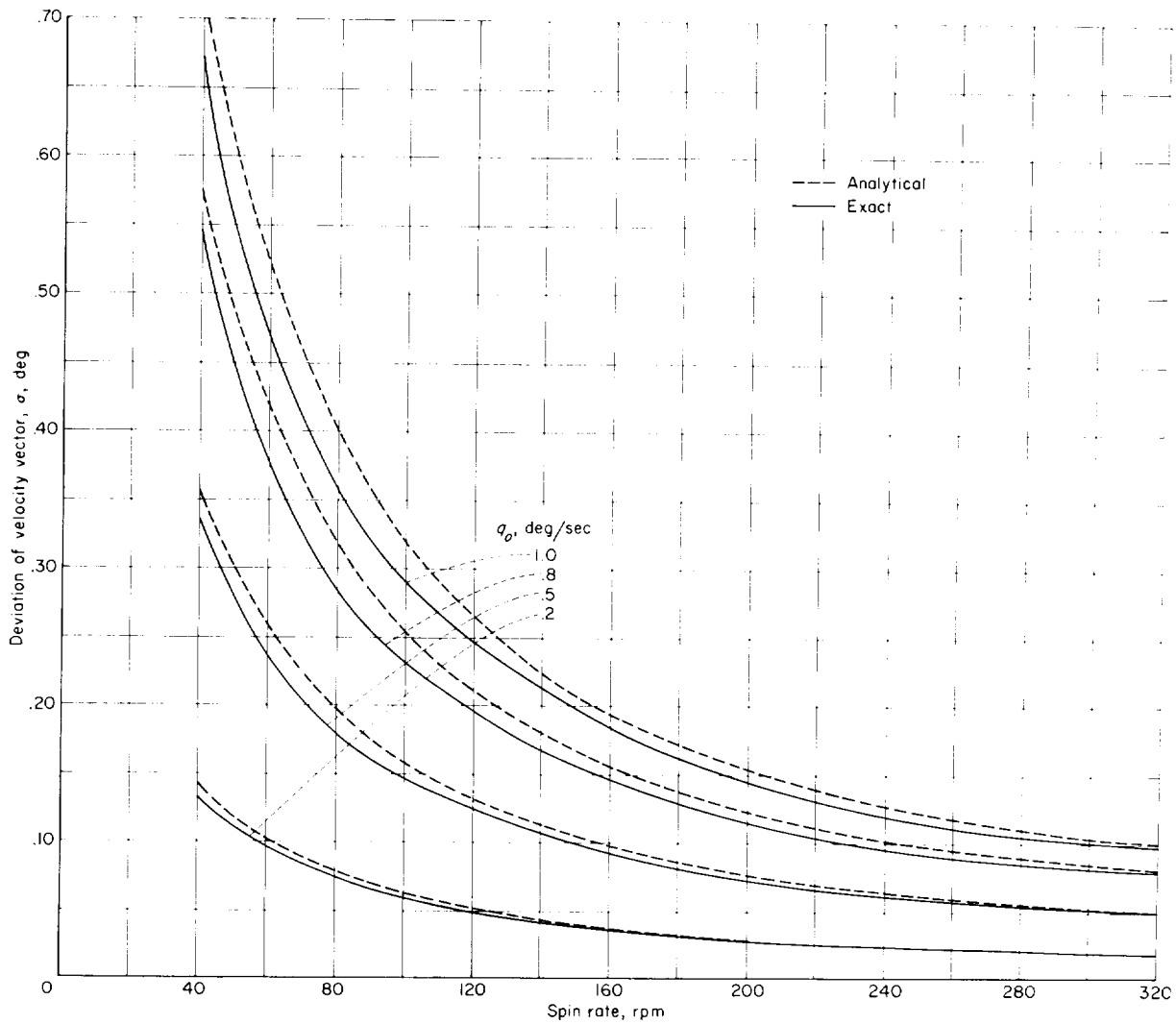


FIGURE 13.- Effect of spin rate on the deviation of the velocity vector due to an initial pitch rate q_0 . Undamped body; $t=30$ seconds (burnout).

unbalance. (See eq. (28).) Since the disturbing moment is proportional to p_o^2 , and since the restoring moment is essentially proportional to $1/p_o^2$, the spin rate does not appear in the parameter determining the magnitude of the disturbance.

Figure 16 is provided to show the deviation of the velocity vector as a function of spin rate for a

spherical rocket motor with characteristics as given in table II. This plot does not include the effect of jet damping. In this motor the ratio I_x/I varies from 0.82 to 0.32.

The figure indicates that caution should be used when the variation in inertia ratio is large. However, even in this extreme case order-of-magnitude numbers can be obtained.

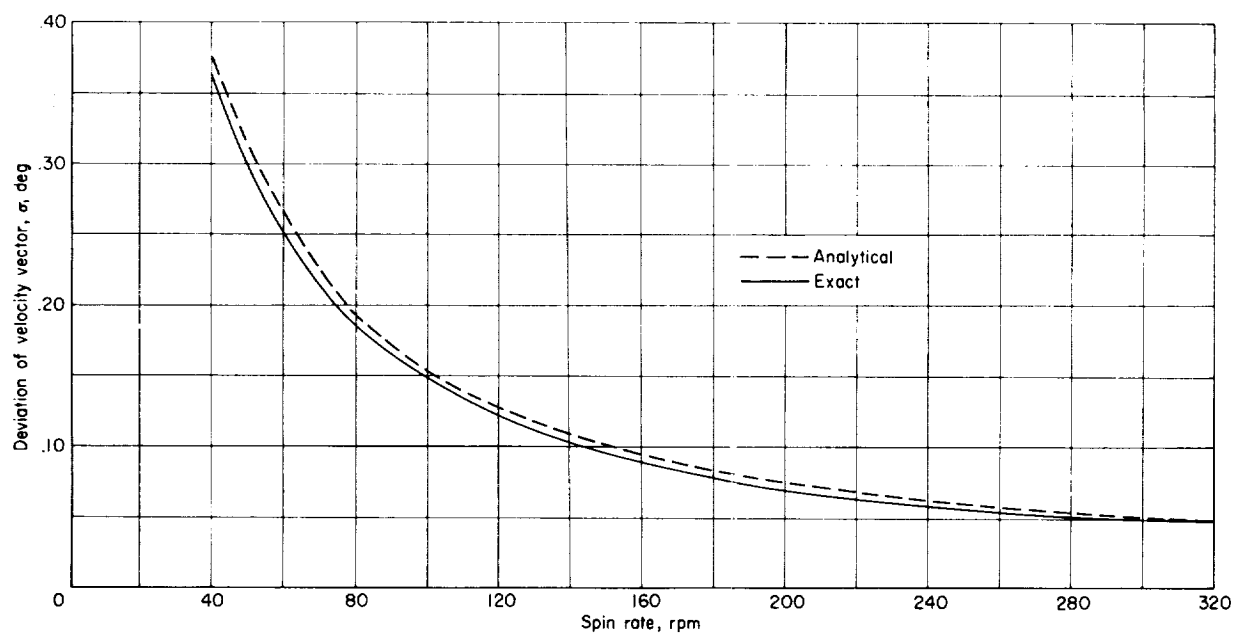


FIGURE 14. Effect of spin rate on the deviation of the velocity vector due to an initial pitch rate q_0 of 0.50 deg/sec. (Damped body; $t = 30$ seconds (burnout)).

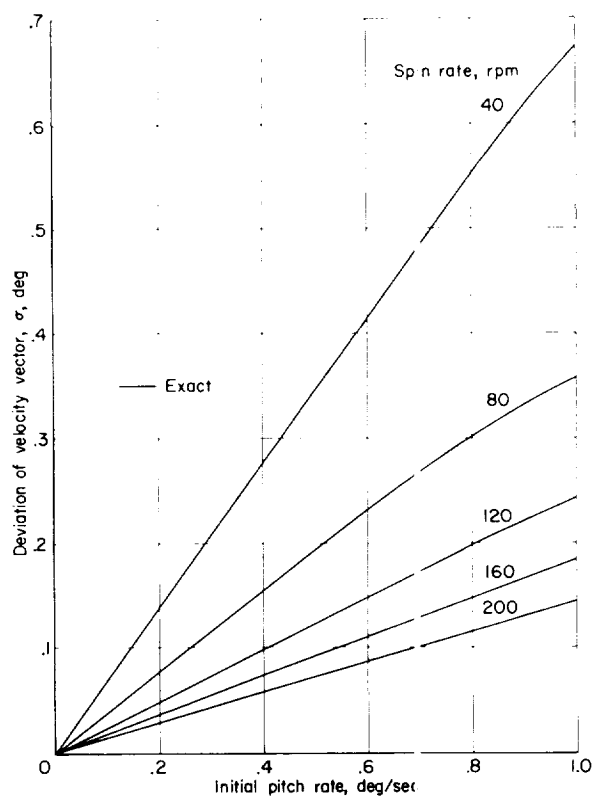


FIGURE 15. Linear effect of initial pitch rate on the deviation of the velocity vector for several spin rates. (Undamped body; $t = 30$ seconds (burnout)).

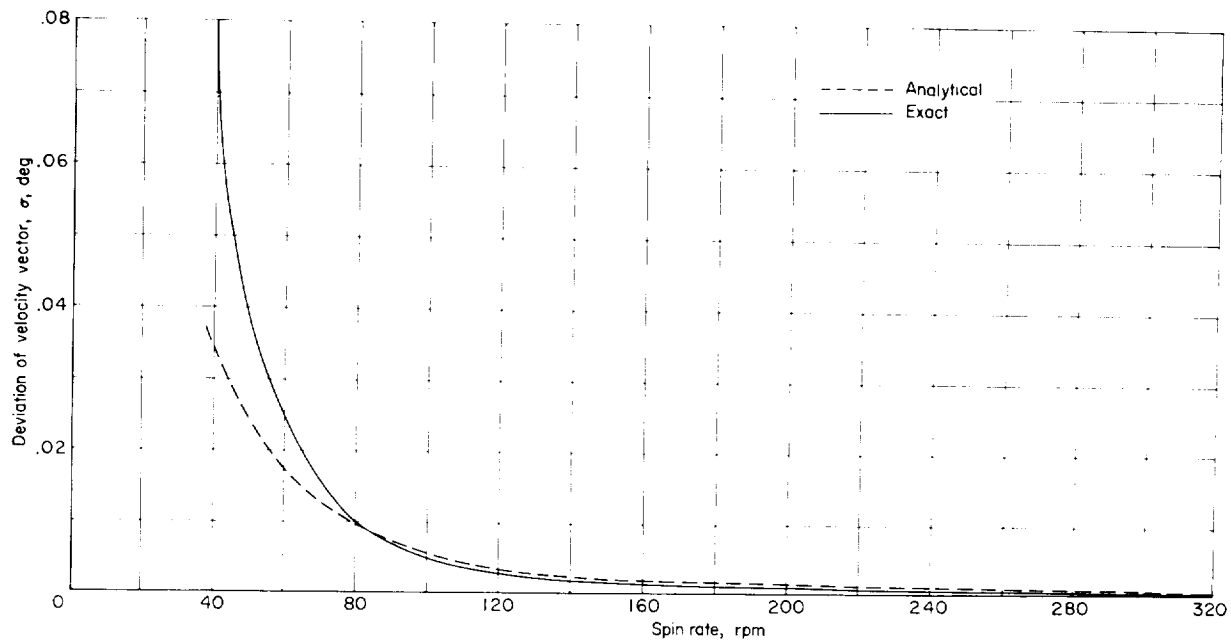


FIGURE 16.—Effect of spin rate on the deviation of the velocity vector due to an applied moment for a 25-inch spherical rocket motor. Undamped body; $t=30$ seconds (burnout).

CONCLUDING REMARKS

The effects of spin stabilization on the flight-path angular deviation caused by initial pitching rate, thrust misalignment, and principal-axis misalignment have been evaluated by an approximate analytical solution which yields the flight-path angular deviation as a function of spin rate for a vehicle whose mass and inertia properties are varying with time. Agreement with a numerical integration of the six-degree-of-freedom equations

of motion was found to be good in all cases in which the inertia ratio was essentially constant.

Spin stabilization was found to be very effective in averaging out the errors caused by initial pitch rates and thrust misalignments, but was completely ineffective in controlling the errors in flight-path angle due to principal-axis misalignment.

LANGLEY RESEARCH CENTER,
NATIONAL AERONAUTICS AND SPACE ADMINISTRATION,
LANGLEY AIR FORCE BASE, VA., April 21, 1961.

APPENDIX

EQUATIONS OF MOTION IN BODY-FIXED AXIS SYSTEM

The symbols used in this appendix are defined as follows:

F_X, F_Y, F_Z	components of external force along the body X-, Y-, and Z-axis, respectively, lb
I_X, I_Y, I_Z	moments of inertia about body X-, Y-, and Z-axis, respectively, slug-ft ²
I_{XZ}	product of inertia, slug-ft ²
I	I_Y or I_Z (where $I_Y = I_Z$), slug-ft ²
l_i, m_i, n_i	direction cosines between inertial axes and body-fixed axes, $i=1, 2, \text{ or } 3$
M_X, M_Y, M_Z	external moments about body X-, Y-, and Z-axis, respectively, ft-lb
m	mass of vehicle, slugs
p, q, r	angular-velocity components of vehicle about body X-, Y-, and Z-axis, respectively, radians/sec
r_e, X	longitudinal distance from vehicle center of gravity to jet exit, ft
$[T_1], [T_2], [T_3]$	transformation matrices
u, v, w	velocity components of vehicle along X-, Y-, and Z-axis, respectively, ft/sec
\mathbf{V}	vehicle velocity vector, ft/sec
$\bar{X}, \bar{Y}, \bar{Z}$	orthogonal body-axis system
$\bar{x}, \bar{y}, \bar{z}$	coordinates of center of gravity of vehicle along \bar{X} -, \bar{Y} -, and \bar{Z} -axis, respectively, ft
$\bar{X}, \bar{Y}, \bar{Z}$	fixed orthogonal axis system, coincident with body-axis system at zero time
γ	orientation of velocity vector in vertical plane, radians
θ	pitch Euler angle, radians (except as noted)
λ	orientation of velocity vector in horizontal plane, radians
σ	total orientation of velocity vector, radians (except as noted)

ϕ roll Euler angle, radians (except as noted)

ψ yaw Euler angle, radians (except as noted)

A dot over a quantity denotes differentiation with respect to time.

The rigid-body equations of motion as programmed on the IBM 704 electronic computer are the standard six-degree-of-freedom equations of motion found in most aeronautical textbooks on dynamic stability (for example, ref. 3, eqs. (10-11)), with damping in pitch and yaw added to the second and third moment equations, respectively. These equations are repeated here for reference. The three force equations are

$$m(\dot{u} - vr + wq) = \sum F_X \quad (\text{A1})$$

$$m(\dot{v} - wp + ur) = \sum F_Y \quad (\text{A2})$$

$$m(\dot{w} - uq + rp) = \sum F_Z \quad (\text{A3})$$

and the moment equations including jet damping are

$$I_X \dot{p} - I_{XZ} \dot{r} + (I_Z - I_Y)qr - I_{XZ}pq = \sum M_X \quad (\text{A4})$$

$$I_Y \dot{q} + (I_Y - I_Z)rp + I_{XZ}(p^2 - r^2) + \dot{I}_Y q + \dot{m}r_{e,X}^2 q = \sum M_Y \quad (\text{A5})$$

$$I_Z \dot{r} - I_{XZ} \dot{p} + (I_Y - I_X)pq + I_{XZ}qr + I_Z r + \dot{m}r_{e,X}^2 r = \sum M_Z \quad (\text{A6})$$

The quantities used here are referred to a set of axes fixed to and rolling with the body, whereas the analysis in the body of this paper is referred to a set of nonrolling axes.

The quantities u , v , w and p , q , r are found by integration of these equations by the Runge-Kutta method, and are then transformed to a set of inertial axes. The following assumptions are made to simplify the integration:

Moments and products of inertia vary linearly with time

Mass varies linearly with time

Damping coefficients $(\dot{m}v_{e,x}^2 + \dot{I})$ are constant

The inertial quantities are found by means of the following transformation equations (ref. 4):

$$\begin{bmatrix} \dot{x} \\ \dot{y} \\ \dot{z} \end{bmatrix} = [T_1][T_2][T_3] \begin{bmatrix} u \\ v \\ w \end{bmatrix} \quad (\text{A7})$$

where the transformation matrices $[T_1]$, $[T_2]$, and $[T_3]$ are given by

$$[T_1] = \begin{bmatrix} \cos \psi & -\sin \psi & 0 \\ \sin \psi & \cos \psi & 0 \\ 0 & 0 & 1 \end{bmatrix} \quad (\text{A8})$$

$$[T_2] = \begin{bmatrix} \cos \theta & 0 & \sin \theta \\ 0 & 1 & 0 \\ -\sin \theta & 0 & \cos \theta \end{bmatrix} \quad (\text{A9})$$

$$[T_3] = \begin{bmatrix} 1 & 0 & 0 \\ 0 & \cos \phi & -\sin \phi \\ 0 & \sin \phi & \cos \phi \end{bmatrix} \quad (\text{A10})$$

Multiplying the matrices gives equation (A7) as

$$\begin{bmatrix} \dot{x} \\ \dot{y} \\ \dot{z} \end{bmatrix} = \begin{bmatrix} l_1 & m_1 & n_1 \\ l_2 & m_2 & n_2 \\ l_3 & m_3 & n_3 \end{bmatrix} \begin{bmatrix} u \\ v \\ w \end{bmatrix} \quad (\text{A11})$$

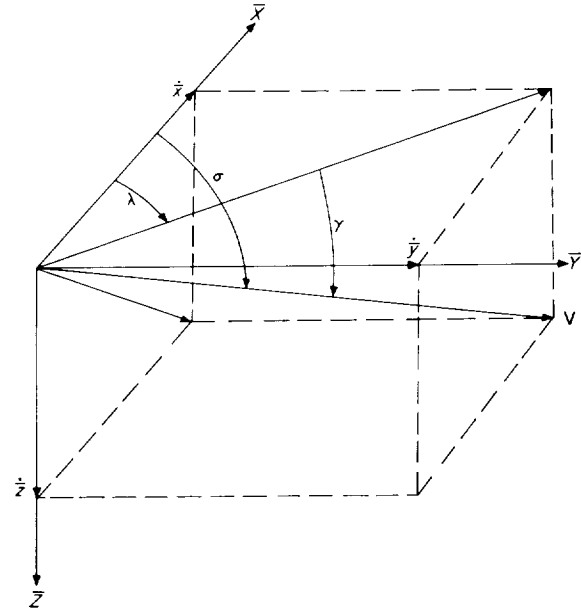
where

$$\left. \begin{aligned} l_1 &= \cos \psi \cos \theta \\ l_2 &= \sin \psi \cos \theta \\ l_3 &= -\sin \theta \\ m_1 &= \cos \psi \sin \theta \sin \phi - \sin \psi \cos \phi \\ m_2 &= \sin \psi \sin \theta \sin \phi + \cos \psi \cos \phi \\ m_3 &= \cos \theta \sin \phi \\ n_1 &= \cos \psi \sin \theta \cos \phi + \sin \psi \sin \phi \\ n_2 &= \sin \psi \sin \theta \cos \phi - \cos \psi \sin \phi \\ n_3 &= \cos \theta \cos \phi \end{aligned} \right\} \quad (\text{A12})$$

The angular rates p, q, r about the body axes are transformed to angular rates $\dot{\phi}, \dot{\theta}, \dot{\psi}$ about the space axes by means of the following transformations (ref. 4):

$$\left. \begin{aligned} \dot{\phi} &= p + \tan \theta (q \sin \phi + r \cos \phi) \\ \dot{\theta} &= q \cos \phi - r \sin \phi \\ \dot{\psi} &= \frac{1}{\cos \theta} (q \sin \phi + r \cos \phi) \end{aligned} \right\} \quad (\text{A13})$$

Application of these transformations to the body-axis quantities u, v, w and p, q, r yields time histories of $\dot{x}, \dot{y}, \dot{z}$ and ϕ, θ, ψ . Then, from sketch 2, γ, λ , and σ can be found:



Sketch 2.

Thus,

$$\left. \begin{aligned} \gamma &= \tan^{-1} \frac{\dot{z}}{\sqrt{\dot{x}^2 + \dot{y}^2}} \\ \lambda &= \tan^{-1} \frac{\dot{y}}{\dot{x}} \\ \sigma &= \tan^{-1} \frac{\sqrt{\dot{x}^2 + \dot{y}^2}}{\dot{x}} \end{aligned} \right\} \quad (\text{A14})$$

REFERENCES

1. Nicolaides, John D.: On the Free Flight Motion of Missiles Having Slight Configurational Asymmetries. Rep. No. 858, Ballistic Res. Labs., Aberdeen Proving Ground, June 1953.
2. Jarmolow, Kenneth: Dynamics of a Spinning Rocket With Varying Inertia and Applied Moment. Jour. Appl. Phys., vol. 28, no. 3, Mar. 1957, pp. 308-313.
3. Perkins, Courtland D., and Hage, Robert E.: Airplane Performance Stability and Control. John Wiley & Sons, Inc., c.1949.
4. Abzug, Malcolm J.: Applications of Matrix Operators to the Kinematics of Airplane Motion. Jour. Aero. Sci. vol. 23, no. 7, July 1956, pp. 679-684.